Clim. Past, 19, 1265–1274, 2023
https://doi.org/10.5194/cp-19-1265-2023


Climate of the Past
Open Access
EGU

# Technical note: A new online tool for $\delta^{18}$O–temperature conversions

**Daniel E. Gaskell**[1] **and Pincelli M. Hull**[2]

[1]Department of Earth and Planetary Sciences, University of California Santa Cruz, Santa Cruz, CA 95064, USA
[2]Department of Earth and Planetary Sciences, Yale University, New Haven, CT 06511, USA

**Correspondence:** Daniel E. Gaskell (daniel.gaskell@yale.edu)

Received: 23 September 2022 – Discussion started: 11 October 2022
Revised: 30 March 2023 – Accepted: 29 April 2023 – Published: 22 June 2023

**Abstract.** The stable-oxygen-isotopic composition of marine carbonates ($\delta^{18}O_c$) is one of the oldest and most widely used paleothermometers. However, interpretation of these data is complicated by the necessity of knowing the $\delta^{18}O$ of the source seawater ($\delta^{18}O_w$) from which $CaCO_3$ is precipitated. The effect of local hydrography (the "salinity effect") is particularly difficult to correct for and may lead to errors of $> 10\,^{\circ}C$ in sea-surface temperatures if neglected. A variety of methods for calculating $\delta^{18}O_w$ have been developed in the literature, but not all are readily accessible to workers. Likewise, temperature estimates are sensitive to a range of other calibration choices (such as calibration species and the inclusion or exclusion of carbonate ion effects), which can require significant effort to intercompare. We present an online tool for $\delta^{18}O$–temperature conversions which provides convenient access to a wide range of calibrations and methods from the literature. Our tool provides a convenient way for workers to examine the effects of alternate calibration and correction procedures on their $\delta^{18}O$-based temperature estimates.

## 1 Motivation

The stable-oxygen-isotopic composition of carbonates ($\delta^{18}O_c$) is one of the oldest and most widely used paleothermometers and undergirds a wide variety of paleoceanographic research (for recent reviews, see Pearson, 2012, and Sharp, 2017). Converting $\delta^{18}O_c$ to temperature is typically done using an empirical calibration in either a linear form, such as

$$T = 16.5 - 4.80\left(\delta^{18}O_c - \delta^{18}O_w - 0.27\right), \quad (1)$$

(Bemis et al., 1998), or in a quadratic form, such as

$$T = 16.0 - 5.17\left(\delta^{18}O_c - \delta^{18}O_w - 0.20\right) + 0.09\left(\delta^{18}O_c - \delta^{18}O_w - 0.20\right)^2, \quad (2)$$

(McCrea, 1950, as reformulated by Bemis et al., 1998), where $T$ is temperature (in °C), $\delta^{18}O_c$ is the oxygen isotope composition of the carbonate (as ‰ VPDB, or parts per thousand relative to the Vienna Pee Dee Belemnite standard), and $\delta^{18}O_w$ is the oxygen isotope composition of the water in which the carbonate was precipitated (as ‰ VSMOW, or parts per thousand relative to the Vienna Standard Mean Ocean Water standard). Much of the complexity of using $\delta^{18}O$ as a paleothermometer arises from the need to know $\delta^{18}O_w$, which may vary both globally as a function of ice volume and locally at the sea surface as a function of regional hydrography (Rohling, 2013). Global variation can be estimated using independent records of sea level, so the global record of deep-water $\delta^{18}O$-based temperatures has been relatively well established (Zachos et al., 2001; Cramer et al., 2009; Westerhold et al., 2020; Rohling et al., 2021; etc.). However, local variations in surface $\delta^{18}O_w$ are more difficult to predict, rendering sea-surface temperature (SST) estimates from $\delta^{18}O$ less reliable than deep-water temperature estimates. To address this, a variety of methods have been developed in the literature to estimate surface $\delta^{18}O_w$.

Since modern surface $\delta^{18}O_w$ broadly covaries with latitude, a common approach has been to apply the modern latitudinal variation to a sample's paleolatitude (typically using

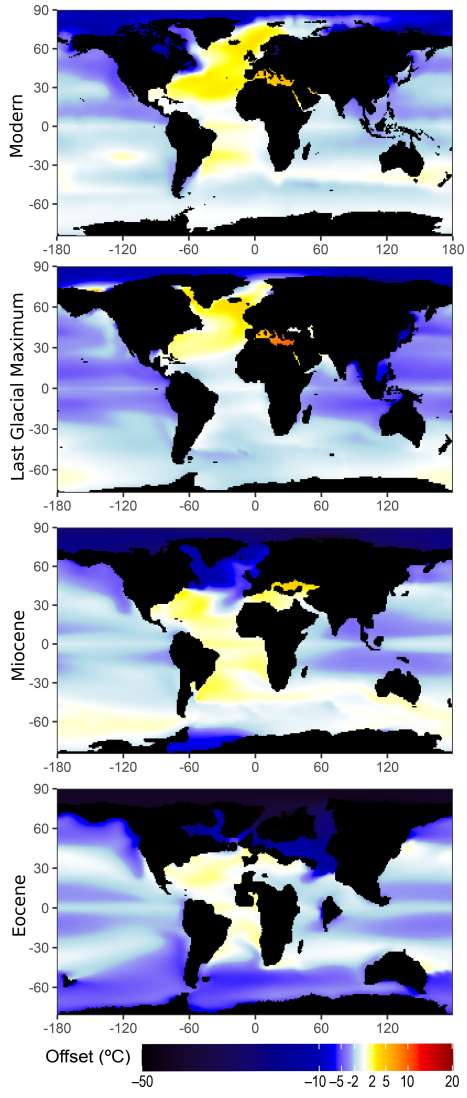


**Figure 1.** Effect of estimating SST using measured/modeled local $\delta^{18}O_w$ rather than the latitude-based approximation of Zachos et al. (1994, Eq. 1 therein). Modern: comparison with mean annual $\delta^{18}O_w$ < 50 m depth (after LeGrande and Schmidt, 2006). Last Glacial Maximum (LGM): comparison with inferred annual surface $\delta^{18}O_w$ at the LGM (Tierney et al., 2020). Miocene: comparison with CESMv1.2_CAM5 model run at 400 ppm $CO_2$ with Miocene paleogeography (Gaskell et al., 2022). Eocene: comparison with CESM_1.2_CAM5 model run at 6 times the preindustrial $CO_2$ with Eocene paleogeography (Zhu et al., 2020). Temperatures are calculated assuming a slope of 4.80 °C ‰$^{-1}$ (Bemis et al., 1998).

the relationship fit from Southern Ocean data in Eq. 1 of Zachos et al., 1994, or more recently the updated method of Hollis et al., 2019). However, this approach performs particularly poorly in the North Atlantic and other high northern latitudes, where local $\delta^{18}O_w$ can deviate significantly from the latitudinal mean (Fig. 1; Zachos et al., 1994; Gaskell et al., 2022; see also generally Tindall et al., 2010). It also assumes that the latitudinal gradient in $\delta^{18}O_w$ has not changed through time, which is contradicted by modeling. In warmer climates with an altered hydrological cycle, models predict that regional salinity contrasts should change due to alterations in the local ratio of evaporation to precipitation (Richter and Xie, 2010; Singh et al., 2016), with an analogous effect on $\delta^{18}O_w$ (Zhou et al., 2008; Tindall et al., 2010; Roberts et al., 2011; Zhu et al., 2020). In particularly extreme cases such as the Eocene, the theoretical difference between modern latitude-derived $\delta^{18}O_w$ (after Zachos et al., 1994, Eq. 1 therein) and modeled local $\delta^{18}O_w$ at 6 times the preindustrial $pCO_2$ (Zhu et al., 2020) yields a mean temperature error of 5 °C in the Southern Ocean (60–90° S) or an astonishing mean temperature error of 41 °C above the Arctic Circle (66.5–90° N; Fig. 1).

An alternative approach is to obtain $\delta^{18}O_w$ more or less directly from isotope-enabled climate models (Zhou et al., 2008; Roberts et al., 2011; Gaskell et al., 2022). Several approaches have been adopted: drawing local $\delta^{18}O_w$ directly from model output (Roberts et al., 2011); using modeled zonal mean $\delta^{18}O_w$ for a particular paleolatitude (Zhou et al., 2008); using models as input to fit a generalized equation for predicting $\delta^{18}O_w$ from latitude and bottom-water temperature (Gaskell et al., 2022 Eq. S9); or, recently, a generalized method which uses bottom-water temperature to interpolate local $\delta^{18}O_w$ between models run at different $pCO_2$ (Gaskell et al., 2022). While some authors have avoided these approaches altogether due to the uncertainty in modeled $\delta^{18}O_w$ (e.g., Hollis et al., 2012) or the possibility of introducing circularity into data–model comparisons (e.g., Hollis et al., 2019), model-derived $\delta^{18}O_w$ clearly captures information lost by simpler approaches and is therefore appropriate for some use cases (Roberts et al., 2011).

Here, a new online tool for $\delta^{18}O$ temperature conversion is presented which automates a range of methods for $\delta^{18}O_w$ reconstruction and correction from the literature, improving the accessibility of advanced methods to workers generating $\delta^{18}O_c$ data.

## 2 Description

We present a new online tool for performing $\delta^{18}O_c$–temperature conversions which automates a range of methods from the literature. This tool is available at https://research.peabody.yale.edu/d180/ (last access: 7 June 2023). The general workflow for using the tool is summarized in Fig. 2; details on the methodology and reasoning behind each option are given below.

### 2.1 $\delta^{18}O_c$–temperature calibration

After manually entering or uploading a data sheet of $\delta^{18}O_c$ measurements in .csv format, users may select from 1 of 59 different calibrations from the literature (Bemis et al., 1998; Böhm et al., 2000; Bouvier-Soumagnac and Dup-

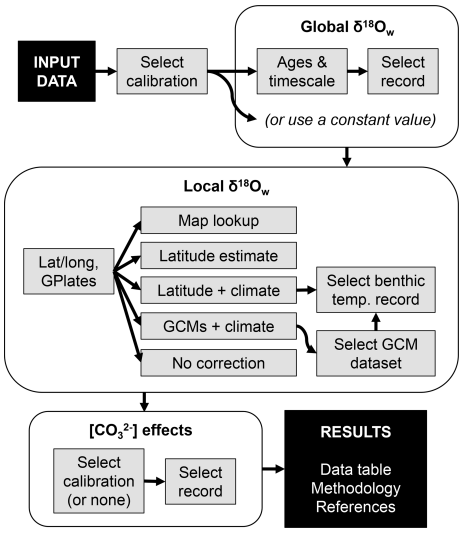


**Figure 2.** General workflow for using the tool. (Each box may reflect multiple sub-options.)

lessy, 1985; Duplessy et al., 2002; Epstein et al., 1953; Erez and Luz, 1983; Farmer et al., 2007; Geffen, 2012; Godiksen et al., 2010; Grossman and Ku, 1986; Høie et al., 2004; Juillet-Leclerc and Schmidt, 2001; Kim and O'Neil, 1997; Kim et al., 2007; Lynch-Stieglitz et al., 1999; Malevich et al., 2019; Marchitto et al., 2014; McCrea, 1950; Mulitza et al., 2003; O'Neil et al., 1969; Patterson et al., 1993; Reynaud-Vaganay et al., 1999; Rosenheim et al., 2009; Shackleton, 1974; Storm-Suke et al., 2007; Thorrold et al., 1997; Tremaine et al., 2011; White et al., 1999; Willmes et al., 2019). All data are expressed with $\delta^{18}O_c$ in units of ‰ VPDB and $\delta^{18}O_w$ in units of ‰ VSMOW, with any standard interconversions expected by the chosen calibration performed automatically. Standard interconversion is notably inconsistent in the literature, with many paleoceanographic papers employing the relationship $\delta^{18}O_{VPDB} = \delta^{18}O_{VSMOW} - 0.27$‰ (Hut, 1987), while many geochemical papers employ the incompatible relationship $\delta^{18}O_{VPDB} = 0.97001 \times \delta^{18}O_{VSMOW} - 29.99$‰ (Brand et al., 2014). The former is actually the isotopic offset between the related VPDB-$CO_2$ and VSMOW-$CO_2$ scales, but the difference is unimportant so long as all data are treated in the manner the calibration expects, as our tool ensures. A full list of included calibrations and standard conversions is given in Tables 1–3.

Where applicable, we use the standardized reformulations of Bemis et al. (1998) and Willmes et al. (2019) or exact algebraic rearrangements of the original equations. For the bayfox core-top calibrations of Malevich et al. (2019), the standard bayfox tool re-fits the calibration coefficients with every run. Since this is computationally expensive, we instead use the linear calibration coefficients fit by runs of the R package bayfoxr 0.0.1 directly in linear functions of the form of Eq. (1) (see Table 1). These yield results equivalent to the full fitting process within numerical error (mean residual = ±0.02 °C, identical to the mean scatter between replicates of the full bayfox fit).

## 2.2 Global $\delta^{18}O_w$ estimation

Users may specify global $\delta^{18}O_w$ manually or choose to draw $\delta^{18}O_w$ by sample age from 12 different time series of global $\delta^{18}O_w$ from the literature (from Cramer et al., 2011; Henkes et al., 2018; Meckler et al., 2022; Miller et al., 2020; Modestou et al., 2020; Rohling et al., 2021; and Veizer and Prokoph, 2015). These records are typically constructed by assuming that the benthic $\delta^{18}O$ record reflects a combination of temperature and ice volume and then subtracting out an independent record of temperature (e.g., using Mg/Ca-based bottom-water temperatures; Cramer et al., 2011) or ice volume (e.g., using a multi-proxy sea level reconstruction; Rohling et al., 2021) to determine the residual $\delta^{18}O_w$. Which global $\delta^{18}O_w$ record is most realistic remains a contentious topic in the literature, with sea-level and Mg/Ca-based records (e.g., Cramer et al., 2011; Rohling et al., 2021) predicting up to ∼ 1 ‰ lower $\delta^{18}O_w$ for much of the Cenozoic than records based on clumped isotope paleothermometry (Meckler et al., 2022; see also Agterhuis et al., 2022). We provide both classes of record here for comparison by the user.

Records are mapped to the user data's ages by linear interpolation. The Δ47-based $\delta^{18}O_w$ records of Meckler et al. (2022) included in our tool were generated by interpolating the authors' original results to 0.1 Myr resolution using the Monte Carlo LOESS method and parameters described in the original publication (Meckler et al., 2022).

All built-in $\delta^{18}O_w$ and temperature records are internally converted to four different timescales, so the user can select the timescale consistent with their data: GTS2004 (Gradstein et al., 2005), GTS2012 (Gradstein et al., 2012), GTS2016 (Ogg et al., 2016), and GTS2020 (Gradstein et al., 2020). These timescale conversions are performed by linear interpolation between magnetochron boundaries; dataset files can be found on the project GitHub.

## 2.3 Local $\delta^{18}O_w$ estimation

The user may select a method for estimating local $\delta^{18}O_w$. These are as follows: performing no local correction, using modern $\delta^{18}O_w$ from each sample's location and a specified depth (after LeGrande and Schmidt, 2006), using reconstructed Late Holocene or Last Glacial Maximum surface $\delta^{18}O_w$ from each sample's location (model output from Tierney et al., 2020), using $\delta^{18}O_w$ estimated from latitude alone (after Eq. 1 in Zachos et al., 1994, or the method of Hollis et al., 2019), using $\delta^{18}O_w$ estimated from latitude and bottom-water temperature (after Gaskell et al., 2022 Eq. S9), or using $\delta^{18}O_w$ estimated from isotope-enabled climate models (GCMs; after the method of Gaskell et al., 2022, presently

**Table 1.** Linear and quadratic $\delta^{18}$O: temperature calibrations of the form $T = a + b\Delta^{18}O_c + c(\Delta^{18}O_c)^2$, where $\Delta^{18}O_c = \delta^{18}O_c - \delta^{18}O_w$, with the given VSMOW conversion factor first added to $\delta^{18}O_w$ to convert VSMOW into the format expected by the calibration.

| Reference | Material | Method | $a$ | $b$ | $c$ | VSMOW to VPDB | Bounds (°C) | Yield |
|---|---|---|---|---|---|---|---|---|
| Bemis et al. (1998) | *Orbulina universa* high light (HL) | Culture | 14.9 | −4.80 | – | −0.27 ‰ | 15–25 | In situ temperature |
| Bemis et al. (1998) | *Orbulina universa* low light (LL) | Culture | 16.5 | −4.80 | – | −0.27 ‰ | 15–25 | In situ temperature |
| Bemis et al. (1998) | *Orbulina universa* HL + LL mean | Culture | 15.7 | −4.80 | – | −0.27 ‰[a] | 15–25 | In situ temperature for generic photosymbiotic planktonic foraminifera |
| Bemis et al. (1998) | *Globigerina bulloides* (11th chamber) | Culture | 12.6 | −5.07 | – | −0.27 ‰ | 15–24 | In situ temperature |
| Bemis et al. (1998) | *Globigerina bulloides* (12th chamber) | Culture | 13.2 | −4.89 | – | −0.27 ‰ | 15–24 | In situ temperature |
| Bemis et al. (1998) | *Globigerina bulloides* (13th chamber) | Culture | 13.6 | −4.77 | – | −0.27 ‰ | 15–24 | In situ temperature |
| Bouvier-Soumagnac and Duplessy (1985) | *Orbulina universa* | Culture | 16.4 | −4.67 | – | −0.20 ‰[b] | 20–24.6 | In situ temperature |
| Bouvier-Soumagnac and Duplessy (1985) | *Orbulina universa* | Plankton tow regression | 15.4 | −4.81 | – | −0.20 ‰[b] | 20–29.5 | In situ temperature |
| Bouvier-Soumagnac and Duplessy (1985) | *Globorotalia menardii* | Plankton tow regression | 14.6 | −5.03 | – | −0.20 ‰[a] | 22.6–29.2 | In situ temperature |
| Bouvier-Soumagnac and Duplessy (1985) | *Neogloboquadrina dutertrei* | Plankton tow regression | 10.5 | −6.58 | – | −0.20 ‰[a] | 24.6–30.6 | In situ temperature |
| Duplessy et al. (2002) | *Cibicides* spp. | Core-top regression | 12.75 | −3.60 | – | −0.20 ‰[c] | −2 to −13 | Bottom-water temperature |
| Epstein et al. (1953) | Mixed biogenic carbonates | Field sample regression | 16.5 | −4.30 | 0.14 | −0.27 ‰[d] | 7–30 | In situ temperature |
| Erez and Luz (1983) | *Trilobatus sacculifer* | Culture | 17.0 | −4.52 | 0.03 | −0.22 ‰[c] | 14–30 | In situ temperature |
| Farmer et al. (2007) | *Globigerinoides ruber* (white) | Core-top regression | 15.4 | −4.78 | – | −0.27 ‰ | (modern ocean) | Mean annual in situ temperature |
| Farmer et al. (2007) | *Globigerinoides ruber* (pink) | Core-top regression | 14.7 | −4.86 | – | −0.27 ‰ | (modern ocean) | Mean annual in situ temperature |
| Farmer et al. (2007) | *Trilobatus sacculifer* | Core-top regression | 16.2 | −4.94 | – | −0.27 ‰ | (modern ocean) | Mean annual in situ temperature |
| Farmer et al. (2007) | *Orbulina universa* | Core-top regression | 16.5 | −5.11 | – | −0.27 ‰ | (modern ocean) | Mean annual in situ temperature |
| Farmer et al. (2007) | *Pulleniatina obliquiloculata* | Core-top regression | 16.8 | −5.22 | – | −0.27 ‰ | (modern ocean) | Mean annual in situ temperature |
| Farmer et al. (2007) | *Globorotalia menardii* | Core-top regression | 16.6 | −5.20 | – | −0.27 ‰ | (modern ocean) | Mean annual in situ temperature |
| Farmer et al. (2007) | *Neogloboquadrina dutertrei* | Core-top regression | 14.6 | −5.09 | – | −0.27 ‰ | (modern ocean) | Mean annual in situ temperature |
| Farmer et al. (2007) | *Neogloboquadrina tumida* | Core-top regression | 13.1 | −4.96 | – | −0.27 ‰ | (modern ocean) | Mean annual in situ |
| Grossman and Ku (1986) | Mixed molluscs | Core-top regression | 21.8 | −4.69 | – | 0.20 ‰ | 6–22 | Bottom-water temperature |
| Grossman and Ku (1986) | *Hoeglundina elegans* | Core-top regression | 20.6 | −4.38 | – | 0.20 ‰ | 2.5–20 | Bottom-water temperature |

**Table 1.** Continued.

| Reference | Material | Method | a | b | b | VSMOW to VPDB | Bounds (°C) | Yield |
|---|---|---|---|---|---|---|---|---|
| Juillet-Leclerc and Schmidt (2001) | *Porites* spp. | Field sample regression | 9.25 | −4.00 | – | −0.27 ‰[a] | 20–30 | Annual in situ temperature |
| Kim and O'Neil (1997) | Inorganic calcite | Precipitation | 16.1 | −4.64 | 0.09 | −0.27 ‰[b] | 0–40 | In situ temperature |
| Lynch-Stieglitz et al. (1999) | *Cibicidoides* + *Planulina* | Core-top regression | 16.1 | −4.76 | – | −0.27 ‰[a] | 4.1–25.6 | Bottom-water temperature |
| Malevich et al. (2019) | Mixed planktonic foraminifera | Core-top regression | 11.8790 | −4.0562 | – | 0 ‰[e] | 0–29.5 | Mean annual SSTs |
| Malevich et al. (2019) | *Globigerinoides ruber* | Core-top regression | 13.0681 | −5.2605 | – | 0 ‰[e] | 0–29.5 | Mean annual SSTs |
| Malevich et al. (2019) | *Trilobatus sacculifer* | Core-top regression | 12.4053 | −6.3458 | – | 0 ‰[e] | 0–29.5 | Mean annual SSTs |
| Malevich et al. (2019) | *Globigerina bulloides* | Core-top regression | 16.6159 | −4.1291 | – | 0 ‰[e] | 0–29.5 | Mean annual SSTs |
| Malevich et al. (2019) | *Trilobatus sacculifer* | Core-top regression | 12.4053 | −6.3458 | – | 0 ‰[e] | 0–29.5 | Mean annual SSTs |
| Malevich et al. (2019) | *Neogloboquadrina incompta* | Core-top regression | 17.9531 | −5.7401 | – | 0 ‰[e] | 0–29.5 | Mean annual SSTs |
| Malevich et al. (2019) | *Neogloboquadrina incompta* | Core-top regression | 19.8109 | −4.9853 | – | 0 ‰[e] | 0–29.5 | Mean annual SSTs |
| McCrea (1950) | Inorganic calcite | Precipitation | 16.0 | −5.17 | 0.09 | −0.20 ‰[b] | 14–57 | In situ temperature |
| Mulitza et al. (2003) | Mixed planktonic foraminifera | Plankton tow regression | 14.32 | −4.28 | 0.07 | −0.27 ‰ | −2 to 31 | In situ temperature |
| Mulitza et al. (2003) | *Trilobatus sacculifer* | Plankton tow regression | 14.91 | −4.35 | – | −0.27 ‰ | 16–31 | In situ temperature |
| Mulitza et al. (2003) | *Globigerinoides ruber* (white) | Plankton tow regression | 14.20 | −4.44 | – | −0.27 ‰ | 16–31 | In situ temperature |
| Mulitza et al. (2003) | *Globigerina bulloides* | Plankton tow regression | 14.62 | −4.70 | – | −0.27 ‰ | 1–25 | In situ temperature |
| Mulitza et al. (2003) | *Neogloboquadrina pachyderma* | Plankton tow regression | 12.69 | −3.55 | – | −0.27 ‰ | 1–25 | In situ temperature |
| O'Neil et al. (1969) | Inorganic calcite | Precipitation | 16.9 | −4.38 | 0.10 | −0.20 ‰[b] | 0–500 | In situ temperature |
| Reynaud-Vaganay et al. (1999) | *Stylophora pistillata* | Culture | 16.15 | −7.69 | – | 1.29 ‰[a] | 21–29 | In situ temperature |
| Reynaud-Vaganay et al. (1999) | *Acropora* spp. | Culture | 19.81 | −3.70 | – | 1.29 ‰[a] | 21–29 | In situ temperature |
| Rosenheim et al. (2009) | *Ceratoporella nicholsoni* | Culture | 16.1 | −6.5 | – | 0 ‰ | 23–27.5 | In situ temperature |
| Shackleton (1974) | *Uvigerina* spp. | Core-top regression | 16.9 | −4.0 | – | −0.20 ‰[b] | 0.8–7 | Bottom-water temperature |

[a] Rearranged by this work; [b] reformulated by Bemis et al. (1998); [c] reformulated by Mulitza et al. (2003); [d] reformulated by Bemis et al. (1998), with VSMOW correction after Grossman (2012); [e] reformulated in this work by extracting the linear coefficients from the Bayesian posterior values.

**Table 2.** Logarithmic $\delta^{18}O$: temperature calibrations of the form $1000\ln\alpha = a(10^3 T K^{-1}) - b$, where TK is temperature (in kelvin), and $\alpha$ is the fractionation factor $\alpha = \frac{\delta^{18}O_c+1000}{\delta^{18}O_w+100}$. The temperature solution for this form (in °C) is $T = \frac{a\times10^3}{1000\ln\left(\frac{\delta^{18}O_c+1000}{\delta^{18}O_w+1000}\right)+b} - 273.15$, where the relationship $\delta^{18}O_{VPDB} = 0.97001\,\delta^{18}O_{VSMOW} - 29.99$ (Brand et al., 2014) is first applied to convert $\delta^{18}O_c$ from VPDB to VSMOW or to convert $\delta^{18}O_w$ from VSMOW to VPDB, as required by the calibration. (The value requiring conversion is indicated in the "Convert which" column.)

| Reference | Material | Method | a | b | Convert which | Bounds (°C) | Yield |
|---|---|---|---|---|---|---|---|
| Böhm et al. (2000) | *Ceratoporella nicholsoni* | Field sample regression | 18.45 | 32.54 | $\delta^{18}O_w$ | 3–28 | In situ temperature |
| Geffen (2012) | *Pleuronectes platessa* otoliths | Culture | 15.99 | 24.25 | $\delta^{18}O_w$ | 11–17 | In situ temperature |
| Godiksen et al. (2010) | *Salvelinus alpinus* otoliths | Culture | 20.43 | 41.14 | $\delta^{18}O_w$ | 2–14* | In situ temperature |
| Høie et al. (2004) | *Gadus morhua* otoliths | Culture | 16.75 | 27.09 | $\delta^{18}O_w$ | 6–20 | In situ temperature |
| Kim et al. (2007) | Inorganic aragonite | Precipitation | 17.88 | 31.14 | $\delta^{18}O_c$ | 0–40 | In situ temperature |
| Patterson et al. (1993) | Mixed freshwater lake fish | Field sample regression | 18.56 | 33.49 | $\delta^{18}O_w$ | 3.2–30.3 | In situ temperature |
| Storm-Suke et al. (2007) | *Salvelinus* spp. otoliths | Field sample regression | 20.69 | 41.69 | $\delta^{18}O_w$ | 2.3–11.8 | In situ temperature |
| Thorrold et al. (1997) | *Micropogonias undulatus* otoliths | Culture | 18.57 | 32.54 | $\delta^{18}O_w$ | 18.2–25* | In situ temperature |
| Tremaine et al. (2011) | Speleothem calcite | Field sample regression | 16.1 | 24.6 | $\delta^{18}O_w$ | 16–21.5 | In situ temperature |
| White et al. (1999) | *Lymnaea peregra* | Culture | 16.74 | 26.39 | $\delta^{18}O_w$ | 8–24 | In situ temperature |
| Willmes et al. (2019) | *Hypomesus transpacificus* otoliths | Culture | 18.39 | 34.56 | $\delta^{18}O_w$ | 16.4–20.5 | In situ temperature |

* Reformulated by Willmes et al. (2019).

**Table 3.** $\delta^{18}O$: temperature calibrations in other forms. $\Delta^{18}O_c = \delta^{18}O_c - \delta^{18}O_w$; the VSMOW–VPDB conversion is included in the equations below, with no further conversion required.

| Reference | Material | Method | Equation | Bounds (°C) | Yield |
|---|---|---|---|---|---|
| Marchitto et al. (2014) | *Cibicidoides* + *Planulina* | Core-top regression | $T = \frac{0.245-\sqrt{0.045461+0.0044\Delta^{18}O_c}}{0.0022}$ | −0.6 to 25.6 | Bottom-water temperature |
| Marchitto et al. (2014) | *Uvigerina peregrina* | Core-top regression | $T = \frac{0.242-\sqrt{0.046468+0.0032\Delta^{18}O_c}}{0.0016}$ | −1.5 to 16.9* | Bottom-water temperature |
| Marchitto et al. (2014) | *Uvigerina* spp. | Core-top regression | Recommended method: subtract 0.47 ‰ from $\delta^{18}O_c$ and use *Cibicidoides* Eq. above | | Bottom-water temperature |
| Marchitto et al. (2014) | *Hoeglundina elegans* | Core-top regression | $T = \frac{0.242-\sqrt{0.053176+0.0012\Delta^{18}O_c}}{0.0006}$ | 2.6–25.6* | Bottom-water temperature |

* Rearranged by this work.

provided using the datasets of Miocene and Eocene paleogeography used in that publication).

For methods which draw from an existing dataset of $\delta^{18}O_w$, the user may specify a number of degrees latitude/-longitude or great-circle radius to average over in order to capture a regional mean when the exact paleocoordinates or local hydrography may not be known. To help determine site locations at the time of deposition, an option is also provided to automatically perform paleocoordinate rotations using the GPlates Web Service (Müller et al., 2018). Ages passed to GPlates are rounded to the nearest 100 ka to reduce the number of calls to the web service.

Our tool does not currently implement any automated consideration of seasonal variation in local $\delta^{18}O_w$, as this is generally treated as negligible by standard methodologies or implicitly baked into the calibration by calibrating against mean annual temperatures and $\delta^{18}O_w$ values (e.g., Malevich et al., 2019).

### 2.4 Carbonate chemistry effects

Because $\delta^{18}O_c$ is known to vary with aqueous carbonate chemistry (the "carbonate ion effect"; Spero et al., 1997; Bijma et al., 1999; Ziveri et al., 2012), users may also specify a carbonate ion correction factor. This is performed by adjusting $\delta^{18}O_c$ with the linear relationship

$$\delta^{18}O_c{}' = \delta^{18}O_c - \left(s\left[CO_3^{2-}\right] - 200s\right), \quad (3)$$

where $\delta^{18}O_c$ is the uncorrected oxygen isotope composition of the carbonate, $\delta^{18}O_c{}'$ is the corrected oxygen isotope composition of the carbonate, $s$ is the selected slope of the effect (in ‰ VPDB per µmol $L^{-1}$ $CO_3^{2-}$), and $[CO_3^{2-}]$ is the concentration of carbonate ion in solution (in µmol $kg^{-1}$). This relationship yields no correction when $[CO_3^{2-}] = 200$ µmol $kg^{-1}$, an approximation of the mean modern surface value (after the long-term record of Zeebe and Tyrrell, 2019). The user may specify $[CO_3^{2-}]$ manually or select a published long-term record of $[CO_3^{2-}]$ (Tyrrell and Zeebe, 2004; Zeebe and Tyrrell, 2019).

### 2.5 Tool output

On completion, the tool presents a formatted table of the resulting temperatures, along with any intermediate values (such as estimated $\delta^{18}O_w$) which were required to generate them. Any rows with potential errors (e.g., paleocoordinates which do not yield a valid $\delta^{18}O_w$ estimate or temperatures which exceed the data range of the calibration) are highlighted in color and flagged with warning text, which appears in an adjacent column. For reference, a short summary of methods is also generated, including relevant equations and a complete bibliography of citations in both text and BibTeX formats for the methods employed in each run.

It should be noted that, while the tool automates the process of applying a given calibration method, the user is still responsible for pre-screening their data for diagenetic alteration or other external biases. For example, use of $\delta^{18}O$ data from foraminifera must consider factors such as diagenetic recrystallization, depth habitat, shell size, and the presence of gametogenic calcite (for a review, see Pearson, 2012).

## 3 Concluding remarks

Our tool provides a convenient way for workers to perform $\delta^{18}O$–temperature conversions and explore the sensitivity of their results to different calibrations, corrections, and $\delta^{18}O_w$ reconstruction methods by successively trying different options in the interface. By allowing data generators to rapidly generate multiple temperature estimates for their records with different underlying assumptions, our tool allows workers to quickly understand and quantify the effects of different assumptions on the resulting temperature estimates.

**Code availability.** An online version of the most current release of our tool is maintained at https://research.peabody.yale.edu/d180/index.html (Gaskell and Hull, 2023a). Source code (JavaScript and PHP) is available from the project's GitHub repository at https://github.com/danielgaskell/d18Oconverter (last access: 13 June 2023) (https://doi.org/10.5281/zenodo.7946599, Gaskell and Hull, 2023b).

**Data availability.** All referenced datasets are included in the source repository for the tool (https://doi.org/10.5281/zenodo.7946599; Gaskell and Hull, 2023b).

**Author contributions.** DEG and PMH conceptualized the tool. DEG wrote the software. DEG and PMH contributed to the manuscript writing.

**Competing interests.** The contact author has declared that neither of the authors has any competing interests.

**Disclaimer.** Publisher's note: Copernicus Publications remains neutral with regard to jurisdictional claims in published maps and institutional affiliations.

**Acknowledgements.** We thank Matthew Huber, Charlotte L. O'Brien, Gordon N. Inglis, R. Paul Acosta, and Christopher J. Poulsen for discussions which contributed to the design of this tool and associated methodologies. We thank Brett Metcalfe and an anonymous referee for their constructive comments, which improved the manuscript. We acknowledge in-

stitutional support from the Yale Peabody Museum and assistance from Nelson Rios in hosting the tool.

**Financial support.** This research has been supported by the National Science Foundation (grant no. 1702851).

**Review statement.** This paper was edited by Marit-Solveig Seidenkrantz and reviewed by Brett Metcalfe and one anonymous referee.

## References

Agterhuis, T., Ziegler, M., de Winter, N. J., and Lourens, L. J.: Warm deep-sea temperatures across Eocene Thermal Maximum 2 from clumped isotope thermometry, Commun. Earth Environ., 3, 1–9, https://doi.org/10.1038/s43247-022-00350-8, 2022.

Bemis, B. E., Spero, H. J., Bijma, J., and Lea, D. W.: Reevaluation of the oxygen isotopic composition of planktonic foraminifera: Experimental results and revised paleotemperature equations, Paleoceanography, 13, 150–160, https://doi.org/10.1029/98PA00070, 1998.

Bijma, J., Spero, H. J., and Lea, D. W.: Reassessing Foraminiferal Stable Isotope Geochemistry: Impact of the Oceanic Carbonate System (Experimental Results), in: Use of Proxies in Paleoceanography, edited by: Fischer, D. G. and Wefer, P. D. G., Springer, Berlin, Heidelberg, 489–512, https://doi.org/10.1007/978-3-642-58646-0_20, 1999.

Böhm, F., Joachimski, M. M., Dullo, W.-C., Eisenhauer, A., Lehnert, H., Reitner, J., and Wörheide, G.: Oxygen isotope fractionation in marine aragonite of coralline sponges, Geochim. Cosmochim. Ac., 64, 1695–1703, https://doi.org/10.1016/S0016-7037(99)00408-1, 2000.

Bouvier-Soumagnac, Y. and Duplessy, J.-C.: Carbon and oxygen isotopic composition of planktonic foraminifera from laboratory culture, plankton tows and Recent sediment; implications for the reconstruction of paleoclimatic conditions and of the global carbon cycle, J. Foraminif. Res., 15, 302–320, https://doi.org/10.2113/gsjfr.15.4.302, 1985.

Brand, W. A., Coplen, T. B., Vogl, J., Rosner, M., and Prohaska, T.: Assessment of international reference materials for isotope-ratio analysis (IUPAC Technical Report), Pure Appl. Chem., 86, 425–467, 2014.

Cramer, B. S., Toggweiler, J. R., Wright, J. D., Katz, M. E., and Miller, K. G.: Ocean overturning since the Late Cretaceous: Inferences from a new benthic foraminiferal isotope compilation, Paleoceanography, 24, PA4216, https://doi.org/10.1029/2008PA001683, 2009.

Cramer, B. S., Miller, K. G., Barrett, P. J., and Wright, J. D.: Late Cretaceous–Neogene trends in deep ocean temperature and continental ice volume: Reconciling records of benthic foraminiferal geochemistry ($\delta^{18}$O and Mg/Ca) with sea level history, J. Geophys. Res.-Oceans, 116, C12023, https://doi.org/10.1029/2011JC007255, 2011.

Duplessy, J.-C., Labeyrie, L., and Waelbroeck, C.: Constraints on the ocean oxygen isotopic enrichment between the Last Glacial Maximum and the Holocene: Paleoceanographic implications, Quaternary Sci. Rev., 21, 315–330, https://doi.org/10.1016/S0277-3791(01)00107-X, 2002.

Epstein, S., Buchsbaum, R., Lowenstam, H. A., and Urey, H. C.: Revised carbonate-water isotopic temperature scale, Geol. Soc. Am. Bull., 64, 1315–1326, 1953.

Erez, J. and Luz, B.: Experimental paleotemperature equation for planktonic foraminifera, Geochim. Cosmochim. Ac., 47, 1025–1031, https://doi.org/10.1016/0016-7037(83)90232-6, 1983.

Farmer, E. C., Kaplan, A., de Menocal, P. B., and Lynch-Stieglitz, J.: Corroborating ecological depth preferences of planktonic foraminifera in the tropical Atlantic with the stable oxygen isotope ratios of core top specimens, Paleoceanography, 22, PA3205, https://doi.org/10.1029/2006PA001361, 2007.

Gaskell, D. E. and Hull, P. M.: $\delta^{18}$O to temperature converter, Yale Peabody Museum, https://research.peabody.yale.edu/d180/index.html (last access: 7 June 2023), 2023a.

Gaskell, D. E. and Hull, P. M.: $\delta^{18}$O to temperature converter, Zenodo [code and data set], https://doi.org/10.5281/zenodo.7946599, 2023b.

Gaskell, D. E., Huber, M., O'Brien, C. L., Inglis, G. N., Acosta, R. P., Poulsen, C. J., and Hull, P. M.: The latitudinal temperature gradient and its climate dependence as inferred from foraminiferal $\delta^{18}$O over the past 95 million years, P. Natl. Acad. Sci. USA, 119, e2111332119, https://doi.org/10.1073/pnas.2111332119, 2022.

Geffen, A. J.: Otolith oxygen and carbon stable isotopes in wild and laboratory-reared plaice (Pleuronectes platessa), Environ. Biol. Fish., 95, 419–430, https://doi.org/10.1007/s10641-012-0033-2, 2012.

Godiksen, J. A., Svenning, M.-A., Dempson, J. B., Marttila, M., Storm-Suke, A., and Power, M.: Development of a species-specific fractionation equation for Arctic charr (Salvelinus alpinus (L.)): an experimental approach, Hydrobiologia, 650, 67–77, https://doi.org/10.1007/s10750-009-0056-7, 2010.

Gradstein, F. M., Ogg, J. G., and Smith, A. G. (Eds.): A Geologic Time Scale 2004, Cambridge University Press, Cambridge, https://doi.org/10.1017/CBO9780511536045, 2005.

Gradstein, F. M., Ogg, J. G., Schmitz, M. D., and Ogg, G. M. (Eds.): The Geologic Time Scale, Elsevier, https://doi.org/10.1016/C2011-1-08249-8, 2012.

Gradstein, F. M., Ogg, J. G., Schmitz, M. D., and Ogg, G. M.: Geologic Time Scale 2020, Elsevier, https://doi.org/10.1016/C2020-1-02369-3, 2020.

Grossman, E. L.: Chapter 10 – Oxygen Isotope Stratigraphy, in: The Geologic Time Scale, edited by: Gradstein, F. M., Ogg, J. G., Schmitz, M. D., and Ogg, G. M., Elsevier, Boston, 181–206, https://doi.org/10.1016/B978-0-444-59425-9.00010-X, 2012.

Grossman, E. L. and Ku, T.-L.: Oxygen and carbon isotope fractionation in biogenic aragonite: Temperature effects, Chem. Geol., 59, 59–74, https://doi.org/10.1016/0168-9622(86)90057-6, 1986.

Henkes, G. A., Passey, B. H., Grossman, E. L., Shenton, B. J., Yancey, T. E., and Pérez-Huerta, A.: Temperature evolution and the oxygen isotope composition of Phanerozoic oceans from carbonate clumped isotope thermometry, Earth Planet. Sc. Lett., 490, 40–50, https://doi.org/10.1016/j.epsl.2018.02.001, 2018.

Høie, H., Otterlei, E., and Folkvord, A.: Temperature-dependent fractionation of stable oxygen isotopes in otoliths of juve-

nile cod (Gadus morhua L.), ICES J. Mar. Sci., 61, 243–251, https://doi.org/10.1016/j.icesjms.2003.11.006, 2004.

Hollis, C. J., Taylor, K. W. R., Handley, L., Pancost, R. D., Huber, M., Creech, J. B., Hines, B. R., Crouch, E. M., Morgans, H. E. G., Crampton, J. S., Gibbs, S., Pearson, P. N., and Zachos, J. C.: Early Paleogene temperature history of the Southwest Pacific Ocean: Reconciling proxies and models, Earth Planet. Sc. Lett., 349–350, 53–66, https://doi.org/10.1016/j.epsl.2012.06.024, 2012.

Hollis, C. J., Dunkley Jones, T., Anagnostou, E., Bijl, P. K., Cramwinckel, M. J., Cui, Y., Dickens, G. R., Edgar, K. M., Eley, Y., Evans, D., Foster, G. L., Frieling, J., Inglis, G. N., Kennedy, E. M., Kozdon, R., Lauretano, V., Lear, C. H., Littler, K., Lourens, L., Meckler, A. N., Naafs, B. D. A., Pälike, H., Pancost, R. D., Pearson, P. N., Röhl, U., Royer, D. L., Salzmann, U., Schubert, B. A., Seebeck, H., Sluijs, A., Speijer, R. P., Stassen, P., Tierney, J., Tripati, A., Wade, B., Westerhold, T., Witkowski, C., Zachos, J. C., Zhang, Y. G., Huber, M., and Lunt, D. J.: The DeepMIP contribution to PMIP4: methodologies for selection, compilation and analysis of latest Paleocene and early Eocene climate proxy data, incorporating version 0.1 of the DeepMIP database, Geosci. Model Dev., 12, 3149–3206, https://doi.org/10.5194/gmd-12-3149-2019, 2019.

Hut, G.: Consultants' group meeting on stable isotope reference samples for geochemical and hydrological investigations, International Atomic Energy Agency, Vienna, Austria, https://inis.iaea.org/search/search.aspx?orig_q=RN:18075746 (last access: 7 June 2023), 1987.

Juillet-Leclerc, A. and Schmidt, G.: A calibration of the oxygen isotope paleothermometer of coral aragonite from Porites, Geophys. Res. Lett., 28, 4135–4138, https://doi.org/10.1029/2000GL012538, 2001.

Kim, S.-T. and O'Neil, J. R.: Equilibrium and nonequilibrium oxygen isotope effects in synthetic carbonates, Geochim. Cosmochim. Ac., 61, 3461–3475, https://doi.org/10.1016/S0016-7037(97)00169-5, 1997.

Kim, S.-T., O'Neil, J. R., Hillaire-Marcel, C., and Mucci, A.: Oxygen isotope fractionation between synthetic aragonite and water: Influence of temperature and $Mg^{2+}$ concentration, Geochim. Cosmochim. Ac., 71, 4704–4715, https://doi.org/10.1016/j.gca.2007.04.019, 2007.

LeGrande, A. N. and Schmidt, G. A.: Global gridded data set of the oxygen isotopic composition in seawater, Geophys. Res. Lett., 33, L12604, https://doi.org/10.1029/2006GL026011, 2006.

Lynch-Stieglitz, J., Curry, W. B., and Slowey, N.: A geostrophic transport estimate for the Florida Current from the oxygen isotope composition of benthic foraminifera, Paleoceanography, 14, 360–373, https://doi.org/10.1029/1999PA900001, 1999.

Malevich, S. B., Vetter, L., and Tierney, J. E.: Global Core Top Calibration of $\delta^{18}$O in Planktic Foraminifera to Sea Surface Temperature, Paleoceanogr. Paleoclimatol., 34, 1292–1315, https://doi.org/10.1029/2019PA003576, 2019.

Marchitto, T. M., Curry, W. B., Lynch-Stieglitz, J., Bryan, S. P., Cobb, K. M., and Lund, D. C.: Improved oxygen isotope temperature calibrations for cosmopolitan benthic foraminifera, Geochim. Cosmochim. Ac., 130, 1–11, https://doi.org/10.1016/j.gca.2013.12.034, 2014.

McCrea, J. M.: On the Isotopic Chemistry of Carbonates and a Paleotemperature Scale, J. Chem. Phys., 18, 849–857, https://doi.org/10.1063/1.1747785, 1950.

Meckler, A. N., Sexton, P. F., Piasecki, A. M., Leutert, T. J., Marquardt, J., Ziegler, M., Agterhuis, T., Lourens, L. J., Rae, J. W. B., Barnet, J., Tripati, A., and Bernasconi, S. M.: Cenozoic evolution of deep ocean temperature from clumped isotope thermometry, Science, 377, 86–90, https://doi.org/10.1126/science.abk0604, 2022.

Miller, K. G., Browning, J. V., Schmelz, W. J., Kopp, R. E., Mountain, G. S., and Wright, J. D.: Cenozoic sea-level and cryospheric evolution from deep-sea geochemical and continental margin records, Sci. Adv., 6, eaaz1346, https://doi.org/10.1126/sciadv.aaz1346, 2020.

Modestou, S. E., Leutert, T. J., Fernandez, A., Lear, C. H., and Meckler, A. N.: Warm Middle Miocene Indian Ocean Bottom Water Temperatures: Comparison of Clumped Isotope and Mg/Ca-Based Estimates, Paleoceanogr. Paleoclimatol., 35, e2020PA003927, https://doi.org/10.1029/2020PA003927, 2020.

Mulitza, S., Boltovskoy, D., Donner, B., Meggers, H., Paul, A., and Wefer, G.: Temperature:$\delta^{18}$O relationships of planktonic foraminifera collected from surface waters, Palaeogeogr. Palaeoclimatol. Palaeoecol., 202, 143–152, https://doi.org/10.1016/S0031-0182(03)00633-3, 2003.

Müller, R. D., Cannon, J., Qin, X., Watson, R. J., Gurnis, M., Williams, S., Pfaffelmoser, T., Seton, M., Russell, S. H. J., and Zahirovic, S.: GPlates: Building a Virtual Earth Through Deep Time, Geochem. Geophy. Geosy., 19, 2243–2261, https://doi.org/10.1029/2018GC007584, 2018.

Ogg, J. G., Ogg, G. M., and Gradstein, F. M.: A Concise Geologic Time Scale, Elsevier, https://doi.org/10.1016/C2009-0-64442-1, 2016.

O'Neil, J. R., Clayton, R. N., and Mayeda, T. K.: Oxygen Isotope Fractionation in Divalent Metal Carbonates, J. Chem. Phys., 51, 5547–5558, https://doi.org/10.1063/1.1671982, 1969.

Patterson, W. P., Smith, G. R., and Lohmann, K. C.: Continental Paleothermometry and Seasonality Using the Isotopic Composition of Aragonitic Otoliths of Freshwater Fishes, in: Climate Change in Continental Isotopic Records, AGU – American Geophysical Union, 191–202, https://doi.org/10.1029/GM078p0191, 1993.

Pearson, P. N.: Oxygen Isotopes in Foraminifera: Overview and Historical Review, The Paleontological Society Papers, 18, 1–38, https://doi.org/10.1017/S1089332600002539, 2012.

Reynaud-Vaganay, S., Gattuso, J.-P., Cuif, J.-P., Jaubert, J., and Juillet-Leclerc, A.: A novel culture technique for scleractinian corals: application to investigate changes in skeletal $\delta^{18}$O as a function of temperature, Mar. Ecol. Prog. Ser., 180, 121–130, https://doi.org/10.3354/meps180121, 1999.

Richter, I. and Xie, S.-P.: Moisture transport from the Atlantic to the Pacific basin and its response to North Atlantic cooling and global warming, Clim. Dynam., 35, 551–566, https://doi.org/10.1007/s00382-009-0708-3, 2010.

Roberts, C. D., LeGrande, A. N., and Tripati, A. K.: Sensitivity of seawater oxygen isotopes to climatic and tectonic boundary conditions in an early Paleogene simulation with GISS ModelE-R, Paleoceanography, 26, PA4203, https://doi.org/10.1029/2010PA002025, 2011.

Rohling, E. J.: Oxygen isotope composition of seawater, in: The Encyclopedia of Quaternary Science, Elsevier, Amsterdam, 915–922, ISBN 978-0-444-53642-6, 2013.

Rohling, E. J., Yu, J., Heslop, D., Foster, G. L., Opdyke, B., and Roberts, A. P.: Sea level and deep-sea temperature reconstructions suggest quasi-stable states and critical transitions over the past 40 million years, Sci. Adv., 7, eabf5326, https://doi.org/10.1126/sciadv.abf5326, 2021.

Rosenheim, B. E., Swart, P. K., and Willenz, P.: Calibration of sclerosponge oxygen isotope records to temperature using high-resolution $\delta^{18}$O data, Geochim. Cosmochim. Ac., 73, 5308–5319, https://doi.org/10.1016/j.gca.2009.05.047, 2009.

Shackleton, N. J.: Attainment of isotopic equilibrium between ocean water and the benthonic foraminifera genus Unigerina: isotopic changes in the ocean during the last glacial, 219, Centre Natl. Rech. Sci. Coll. Inter., 203–209, https://epic.awi.de/id/eprint/32862/ (last access: 7 June 2023), 1974.

Sharp, Z.: Principles of Stable Isotope Geochemistry, 2nd Edn., University of New Mexico Open Textbooks, 416 pp., https://doi.org/10.25844/h9q1-0p82, 2017.

Singh, H. K. A., Donohoe, A., Bitz, C. M., Nusbaumer, J., and Noone, D. C.: Greater aerial moisture transport distances with warming amplify interbasin salinity contrasts, Geophys. Res. Lett., 43, 8677–8684, https://doi.org/10.1002/2016GL069796, 2016.

Spero, H. J., Bijma, J., Lea, D. W., and Bemis, B. E.: Effect of seawater carbonate concentration on foraminiferal carbon and oxygen isotopes, Nature, 390, 497–500, https://doi.org/10.1038/37333, 1997.

Storm-Suke, A., Dempson, J. B., Reist, J. D., and Power, M.: A field-derived oxygen isotope fractionation equation for Salvelinus species, Rapid Commun. Mass Spectrom., 21, 4109–4116, https://doi.org/10.1002/rcm.3320, 2007.

Thorrold, S. R., Campana, S. E., Jones, C. M., and Swart, P. K.: Factors determining $\delta^{13}$C and $\delta^{18}$O fractionation in aragonitic otoliths of marine fish, Geochim. Cosmochim. Ac., 61, 2909–2919, https://doi.org/10.1016/S0016-7037(97)00141-5, 1997.

Tierney, J. E., Zhu, J., King, J., Malevich, S. B., Hakim, G. J., and Poulsen, C. J.: Glacial cooling and climate sensitivity revisited, Nature, 584, 569–573, https://doi.org/10.1038/s41586-020-2617-x, 2020.

Tindall, J., Flecker, R., Valdes, P., Schmidt, D. N., Markwick, P., and Harris, J.: Modelling the oxygen isotope distribution of ancient seawater using a coupled ocean–atmosphere GCM: Implications for reconstructing early Eocene climate, Earth Planet. Sc. Lett., 292, 265–273, https://doi.org/10.1016/j.epsl.2009.12.049, 2010.

Tremaine, D. M., Froelich, P. N., and Wang, Y.: Speleothem calcite farmed in situ: Modern calibration of $\delta^{18}$O and $\delta^{13}$C paleoclimate proxies in a continuously-monitored natural cave system, Geochim. Cosmochim. Ac., 75, 4929–4950, https://doi.org/10.1016/j.gca.2011.06.005, 2011.

Tyrrell, T. and Zeebe, R. E.: History of carbonate ion concentration over the last 100 million years, Geochim. Cosmochim. Ac., 68, 3521–3530, https://doi.org/10.1016/j.gca.2004.02.018, 2004.

Veizer, J. and Prokoph, A.: Temperatures and oxygen isotopic composition of Phanerozoic oceans, Earth-Sci. Rev., 146, 92–104, https://doi.org/10.1016/j.earscirev.2015.03.008, 2015.

Westerhold, T., Marwan, N., Drury, A. J., Liebrand, D., Agnini, C., Anagnostou, E., Barnet, J. S. K., Bohaty, S. M., Vleeschouwer, D. D., Florindo, F., Frederichs, T., Hodell, D. A., Holbourn, A. E., Kroon, D., Lauretano, V., Littler, K., Lourens, L. J., Lyle, M., Pälike, H., Röhl, U., Tian, J., Wilkens, R. H., Wilson, P. A., and Zachos, J. C.: An astronomically dated record of Earth's climate and its predictability over the last 66 million years, Science, 369, 1383–1387, https://doi.org/10.1126/science.aba6853, 2020.

White, R. M. P., Dennis, P. F., and Atkinson, T. C.: Experimental calibration and field investigation of the oxygen isotopic fractionation between biogenic aragonite and water, Rapid Commun. Mass Spectrom., 13, 1242–1247, https://doi.org/10.1002/(SICI)1097-0231(19990715)13:13<1242::AID-RCM627>3.0.CO;2-F, 1999.

Willmes, M., Lewis, L. S., Davis, B. E., Loiselle, L., James, H. F., Denny, C., Baxter, R., Conrad, J. L., Fangue, N. A., Hung, T.-C., Armstrong, R. A., Williams, I. S., Holden, P., and Hobbs, J. A.: Calibrating temperature reconstructions from fish otolith oxygen isotope analysis for California's critically endangered Delta Smelt, Rapid Commun. Mass Spectrom., 33, 1207–1220, https://doi.org/10.1002/rcm.8464, 2019.

Zachos, J., Pagani, M., Sloan, L., Thomas, E., and Billups, K.: Trends, Rhythms, and Aberrations in Global Climate 65 Ma to Present, Science, 292, 686–693, https://doi.org/10.1126/science.1059412, 2001.

Zachos, J. C., Stott, L. D., and Lohmann, K. C.: Evolution of Early Cenozoic marine temperatures, Paleoceanography, 9, 353–387, https://doi.org/10.1029/93PA03266, 1994.

Zeebe, R. E. and Tyrrell, T.: History of carbonate ion concentration over the last 100 million years II: Revised calculations and new data, Geochim. Cosmochim. Ac., 257, 373–392, https://doi.org/10.1016/j.gca.2019.02.041, 2019.

Zhou, J., Poulsen, C. J., Pollard, D., and White, T. S.: Simulation of modern and middle Cretaceous marine $\delta^{18}$O with an ocean-atmosphere general circulation model, Paleoceanography, 23, PA3223, https://doi.org/10.1029/2008PA001596, 2008.

Zhu, J., Poulsen, C. J., Otto-Bliesner, B. L., Liu, Z., Brady, E. C., and Noone, D. C.: Simulation of early Eocene water isotopes using an Earth system model and its implication for past climate reconstruction, Earth Planet. Sc. Lett., 537, 116164, https://doi.org/10.1016/j.epsl.2020.116164, 2020.

Ziveri, P., Thoms, S., Probert, I., Geisen, M., and Langer, G.: A universal carbonate ion effect on stable oxygen isotope ratios in unicellular planktonic calcifying organisms, Biogeosciences, 9, 1025–1032, https://doi.org/10.5194/bg-9-1025-2012, 2012.